Tracking transmitter-gated P2X cation channel activation *in vitro* and *in vivo*

Esther Richler, Severine Chaumont, Eiji Shigetom, Alvaro Sagasti & Baljit S Khakh

Supplementary figures and text:

Supplementary Figure 1. Characterization of $P2X_2$-cam

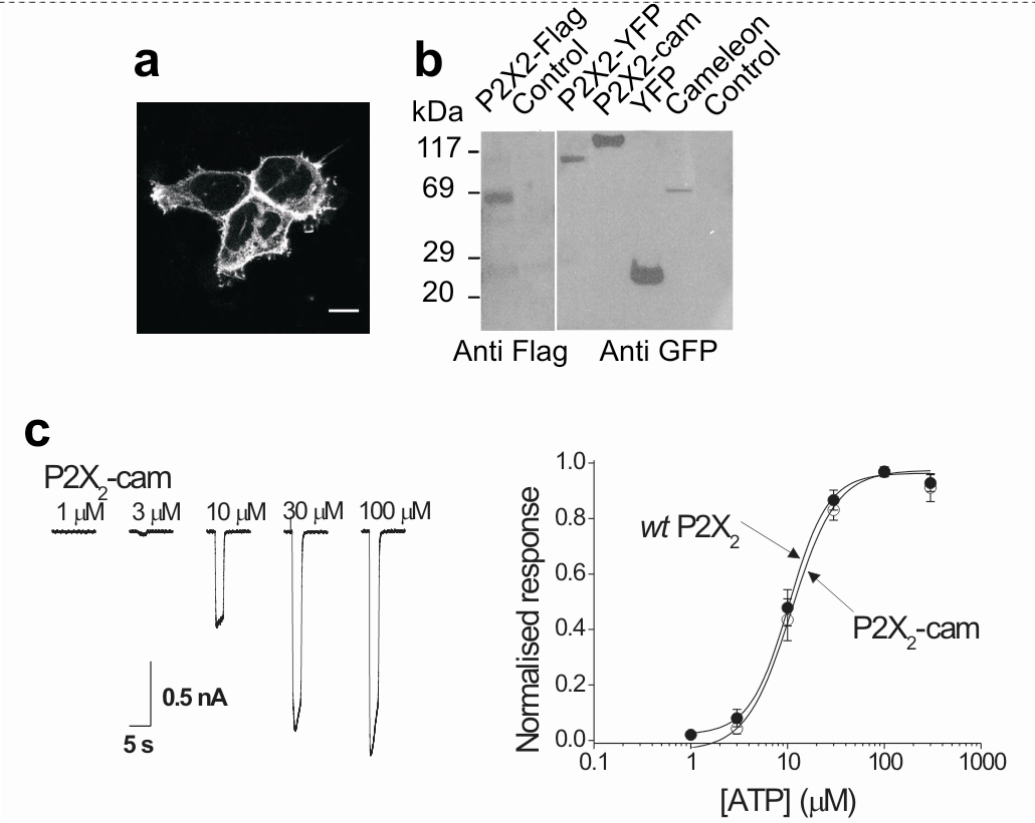

a. Confocal images of 3 HEK cells expressing $P2X_2$-cam receptors (excited at 488 nm, and emission captured at 525 nm; scale bar is 10μm). **b.** Western blot analysis of $P2X_2$ receptor constructs; note there is only one discreet band in each lane. **c.** Representative traces for ATP-evoked currents for $P2X_2$-cam receptors, and ATP concentration response curves for *wt* $P2X_2$ and $P2X_2$-cam receptors.

Supplementary Figure 2. FRET for $P2X_2$-cam.

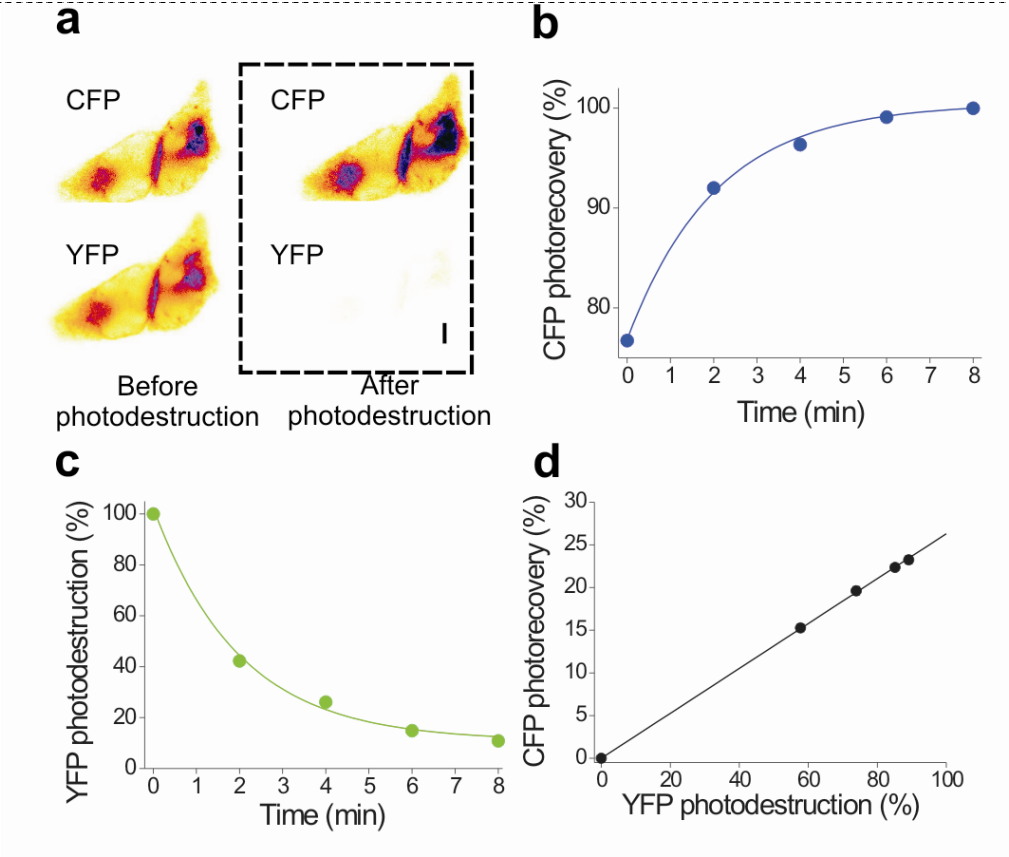

a. Images of HEK cells before and after photodestruction of YFP in $P2X_2$-cam receptors (scale bar is 10μm). **b.** Time course of CFP photorecovery. **c.** Time course of YFP photodestruction. **d.** FRET efficiency for $P2X_2$-cam receptors determined by donor dequenching experiments. In some cases, in this and other figures, the error bars are smaller than the symbol used.

Supplementary Figure 3. Cartoon of the imaging and recording set up.

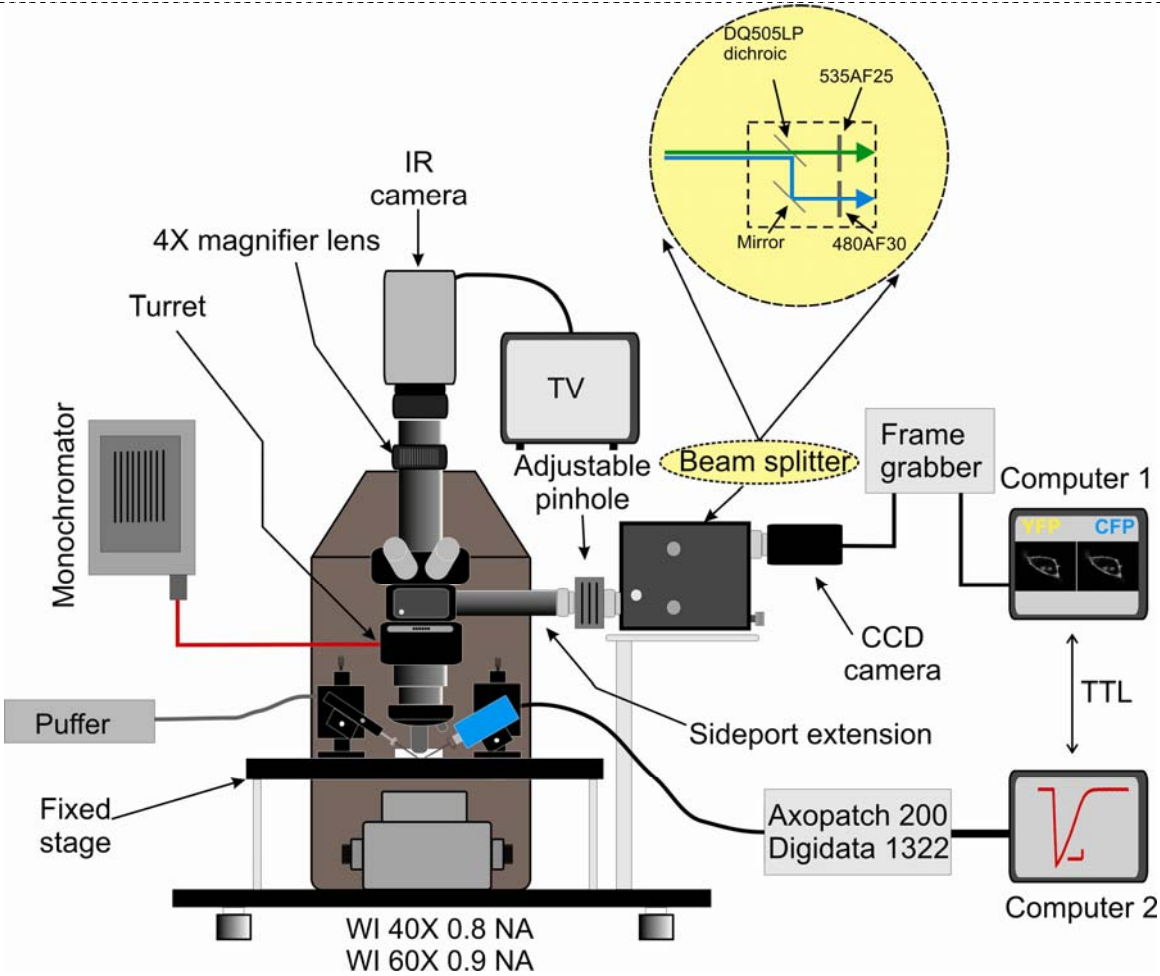

The set up was custom assembled using mostly commercially available components. The puffer (Picospritzer III) was from Intracell, the monochromator (Polychrome IV) from TILL Photonics, the two manipulators (Burleigh PCS6000) from EXFO, the microscope (BX50WI) from Olympus, the 4X magnifier lens from Luigs & Neumann, the fixed stage (MXZP) from Siskiyou Instruments, TV (Monocor CDM-1203) from TILL Photonics, the headstage, Axopatch200 & Digidata 1322 were from Molecular Devices Axon Instruments, the beamsplitter (Optosplit) was from Cairn Instruments, and the IR camera (PCO), CCD camera (Imago) and frame grabber were from TILL Photonics, the side port extension (U-DP1XC) was from Olympus, the PC's were from Dell and the whole set was assembled on an airtable from TMC Corporation. The bath perfusion and suction systems (not shown) were custom made using tubing, clamps and dowel from a hardware store (Home Depot or OSH). Minor electrical components were bought from Radioshack. All the filters in the turret were from Glen Spectra or Omega Optical (see Methods). Further details of the set up, and part numbers, can be obtained from Bal Khakh (bkhakh@mednet.ucla.edu). Bal Khakh would also be happy to help other purinergic labs set up instrumentation similar to ours.

Supplementary Figure 4. P2X$_2$-cam FRET studies by TIRF microscopy.

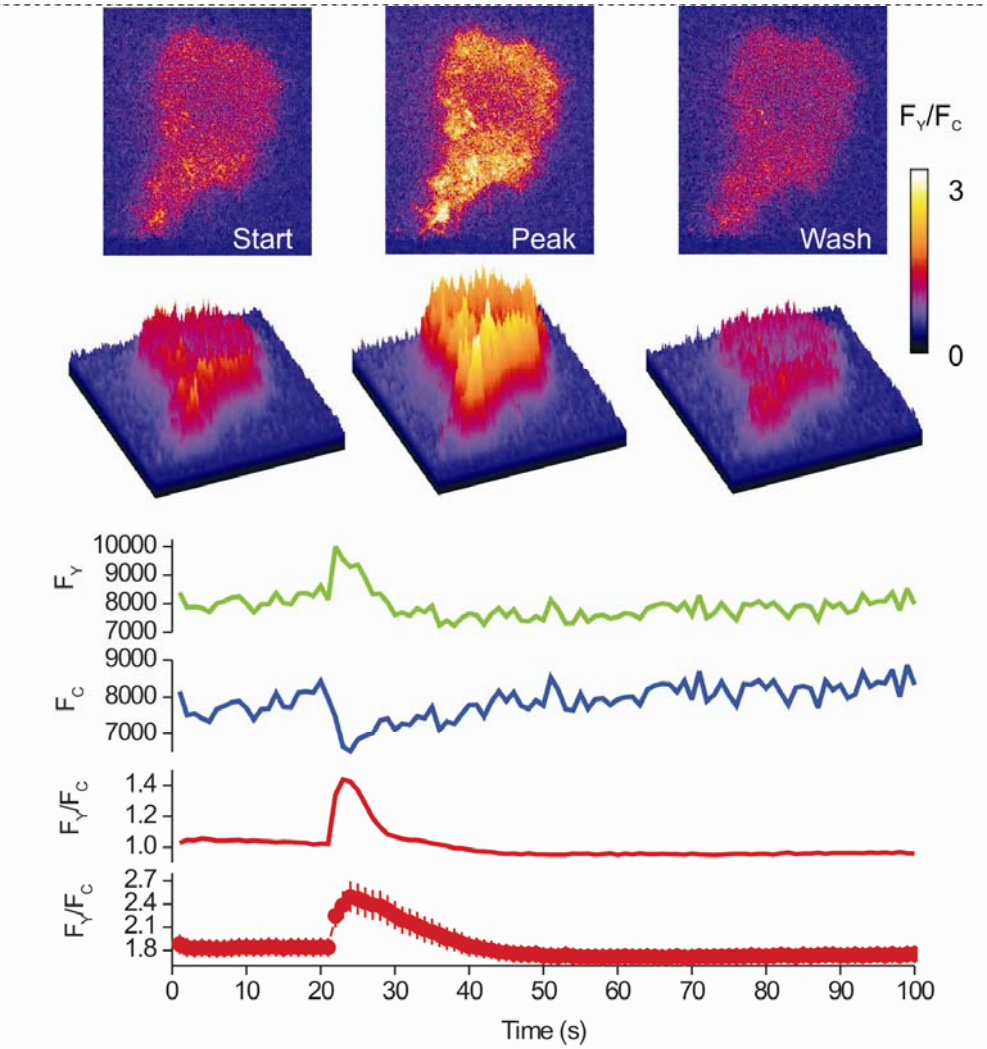

Upper panels shows representative TIRF images before, during and after 100 μM ATP applied to HEK cells expressing P2X$_2$-cam. The lower graph shows representantive and average data for the FRET response evoked by ATP (n = 15).

Supplementary Figure 5. ATP-evoked changes in FRET for all homomeric P2X receptors carrying YC3.1 tags.

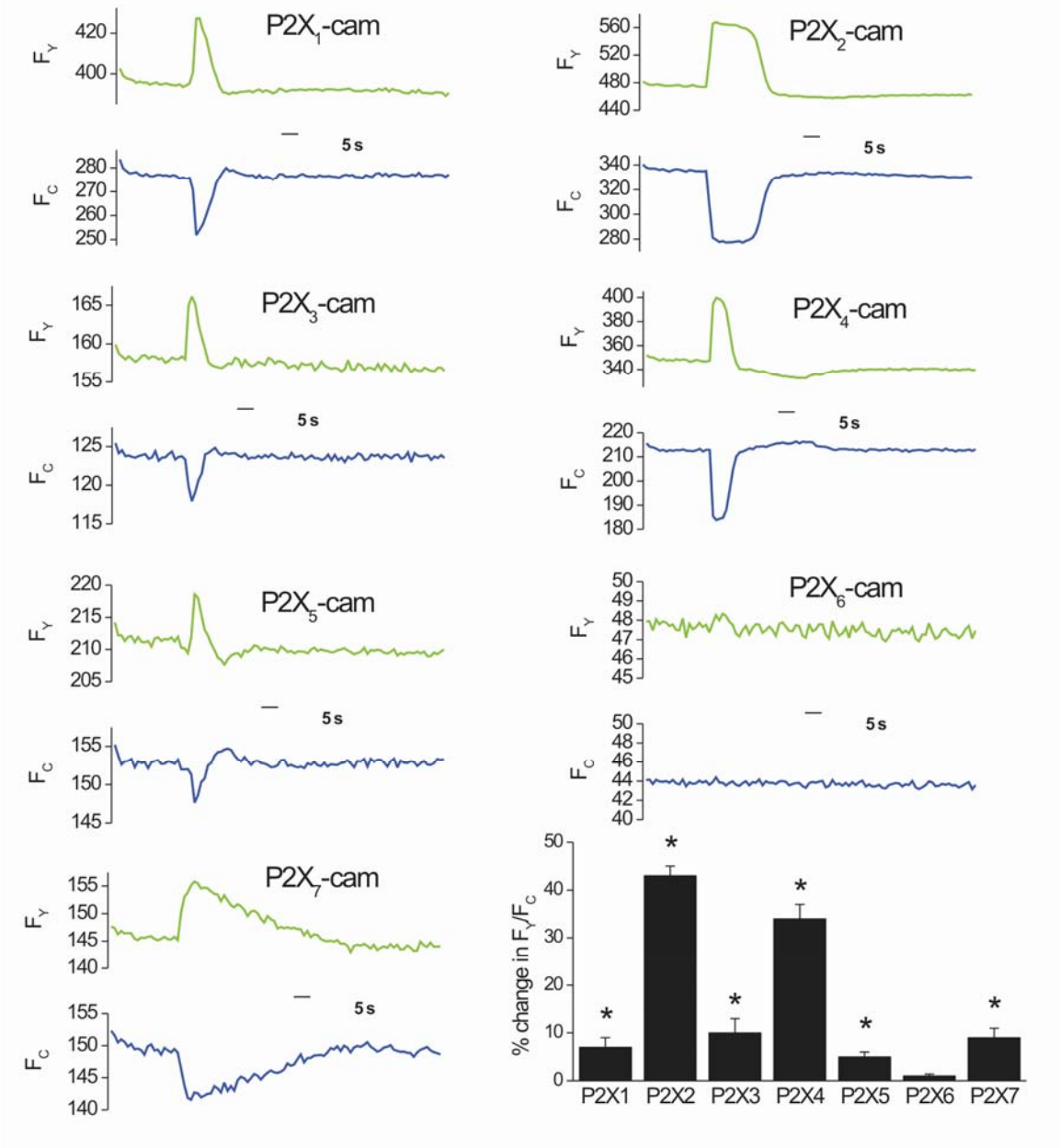

In each case the cells were stimulated with 100 μM ATP at 20 s for 3 s. The exception was $P2X_7$, when 10 μM BzATP was used. In most cases we measured robust increases in F_Y/F_C. $P2X_6$-cam receptors showed no change in F_Y/F_C likely because these channels are non functional. The average data are shown for at least 5 experiments in the bar graph.

Supplementary Figure 6. Biophysical properties of $P2X_2$-cam channels expressed in HEK cells.

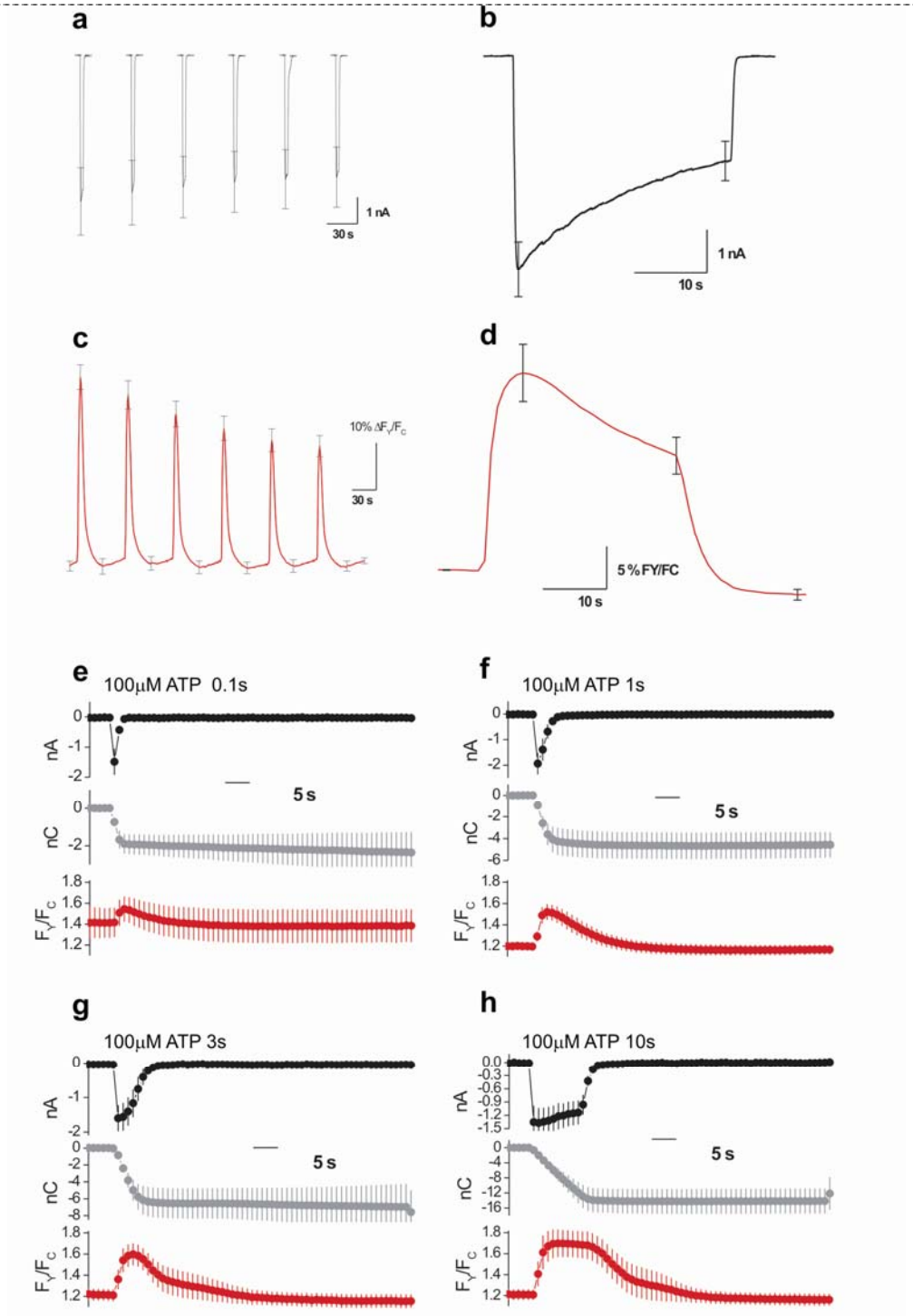

Panels **a** and **c** compare ATP-evoked currents and FRET changes for $P2X_2$-cam receptors expressed in HEK cells and stimulated repetitively with ATP. Panels **b** and **d**, compare ATP-evoked currents and FRET changes for $P2X_2$-cam receptors expressed in HEK cells and stimulated with 30 s applications of ATP. **e-h** Average data for ATP-evoked FRET and current changes in response to different durations of ATP. The middle panels (gray circles) show the integral of the current as charge transfer in nC.

Supplementary Figure 7. FRET for $P2X_2$-cam in neurons.

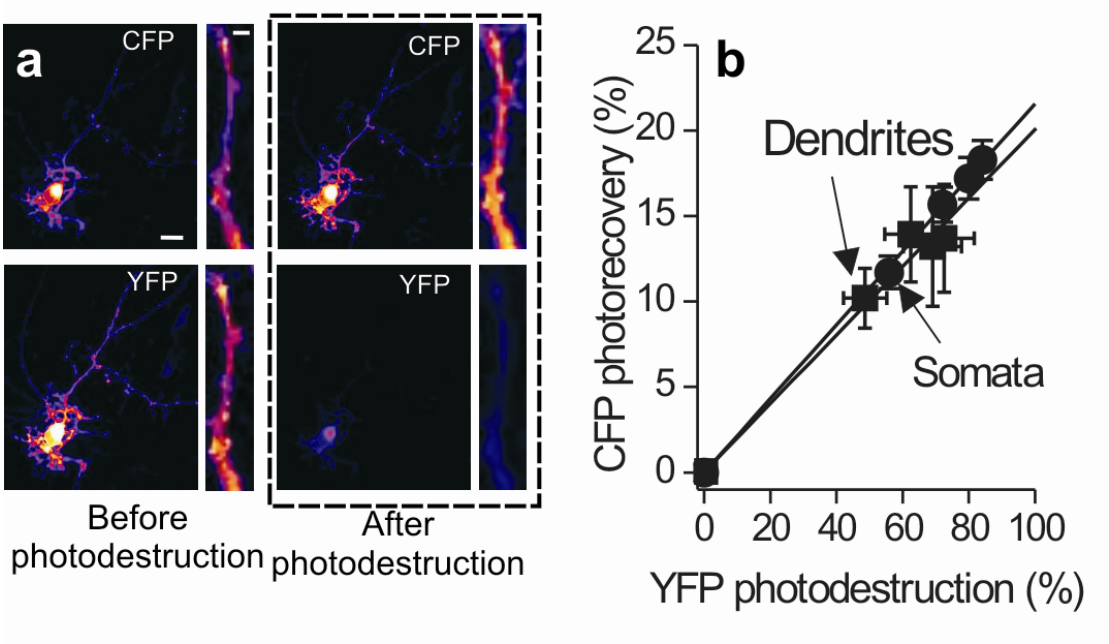

a. Images of a hippocampal neurons (scale 10μm) and dendrite (2μm) before and after photodestruction of YFP in $P2X_2$-cam receptors. **b.** FRET efficiency for $P2X_2$-cam receptors determined by donor dequenching experiments. In some cases, in this and other figures, the error bars are smaller than the symbol used.

Supplementary Figure 8. $P2X_2$-cam channels expressed *in vivo* within zebrafish sensory neurons.

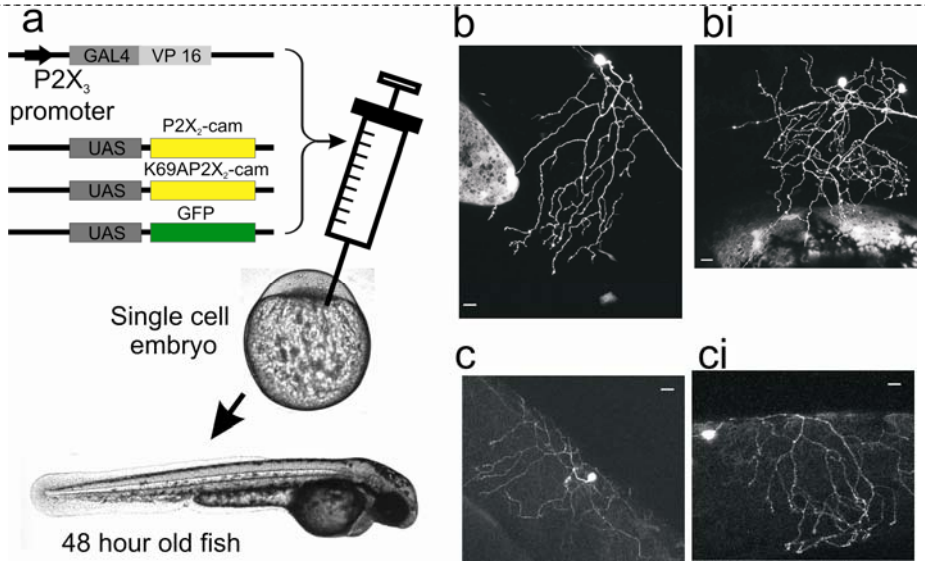

a. The expression strategy. We co-injected a transgene with the *f*$P2X_3$ promoter driving GAL4-VP16 and a transgene with the Gal4 upstream activating sequence (UAS) driving $P2X_2$-cam, GFP or K69A $P2X_2$-cam into zebrafish embryos at the one cell stage. The injected embryos were incubated at 28.5ºC and examined for fluorescence at approximately 48 hours post-fertilization. Fish were anesthetised and immobilised in agar blocks and imaged on a confocal microscope. The images of the fish and embryos are not to scale. The neurons were imaged at 54 hours post fertilisation. **b.** Representative images of neurons expressing GFP. **c.** Representative images of neurons expressing $P2X_2$-cam. In panels B and C the scale bar is 19µm.

Supplementary note 1. Controls for ATP-evoked FRET changes for $P2X_2$-cam receptors.

We carried out a specific set of experiments to examine the relationship between FRET changes for $P2X_2$-cam receptors, and global changes in intracellular Ca^{2+} levels. To this end we recorded FRET changes from single cells, then removed the beam splitter from the emission path of the microscope and measured global Ca^{2+}changes from the cells which had been loaded with Fura-red. We used Fura-red because the emission peak (~660nm) of this organic Ca^{2+} indicator dye (excited at 488nm) does not overlap with that of CFP or YFP and thus can be used in parallel with FRET measurements, from the same cells, without optical interference. We started by studying $P2X_2$-cam receptors (see Fig 1 below). We measured robust ATP-evoked FRET changes for $P2X_2$-cam receptors, as well as robust changes in global Ca^{2+} measured with Fura-red, which decreases in fluorescence intensity when it binds Ca^{2+} (see Fig 1 below). Interestingly however, the FRET change recovered with a time constant (τ) of 6 ± 0.2 s, whereas the global change in Ca^{2+} recovered with a τ of 47±8 s ($P < 0.01$; n = 19). Thus the $P2X_2$-cam FRET signal recovers significantly faster than the global change in Ca^{2+}, providing strong kinetic evidence that the FRET signal does not simply report on global Ca^{2+} levels.

We also pursued another strategy. We co-expressed $P2X_2$-cam receptors with $hP2Y_4$ receptors, because these Gq coupled receptors can be selectively activated with 100 μM UTP and will release Ca^{2+} from intracellular stores[1]. We thus attempted to record FRET from $P2X_2$-cam receptors, while applying UTP to elevate intracellular Ca^{2+} levels. We found that UTP evoked global Ca^{2+} signals equal to those measured with ATP for $P2X_2$-cam receptors (compare panels A & B in Fig 1 below), but we did not measure FRET changes for $P2X_2$-cam receptors, implying that a simple global increase in Ca^{2+} is not responsible for the $P2X_2$-cam FRET signals (see Fig 1). To test this further still we used K69A $P2X_2$-cam receptors in conjunction with *wt*$P2X_4$ receptors. This is because K69A $P2X_2$-cam receptors do not bind ATP and therefore ATP application neither causes FRET nor global Ca^{2+} increases (see Fig 1). Moreover, $P2X_4$ receptors express robustly in HEK cells[2], have the highest fractional calcium currents

among P2X receptors[2] (14%; *versus* 6% for $P2X_2$), and importantly do not form heteromers with $P2X_2$[3]. In essence co-expressing K69A $P2X_2$-cam receptors with *wt* $P2X_4$ allows us to determine if extracellular Ca^{2+} entry through independent $P2X_4$ receptors can cause FRET changes for K69A $P2X_2$-cam receptors. We found that ATP applications to cells co-expressing K69A $P2X_2$-cam and $P2X_4$ receptors caused significant global increases in Ca^{2+} but failed to cause significant increases in FRET for $P2X_2$-cam (see Fig 1). Taken together the data from the TIRF-RET experiments (see main text), from the kinetic analysis (see Fig 1) and from co-expression of $P2X_2$-cam/$hP2Y_4$ and K69A $P2X_2$-cam/$P2X_4$ experiments (see Fig 1) provide strong evidence that the $P2X_2$-cam FRET signals are not simply the result of global Ca^{2+}changes. Previous biochemical characterisation of cytosolic YC3.1, also suggests that this indicator only responded to relatively large Ca^{2+} transients above basal_levels[4].

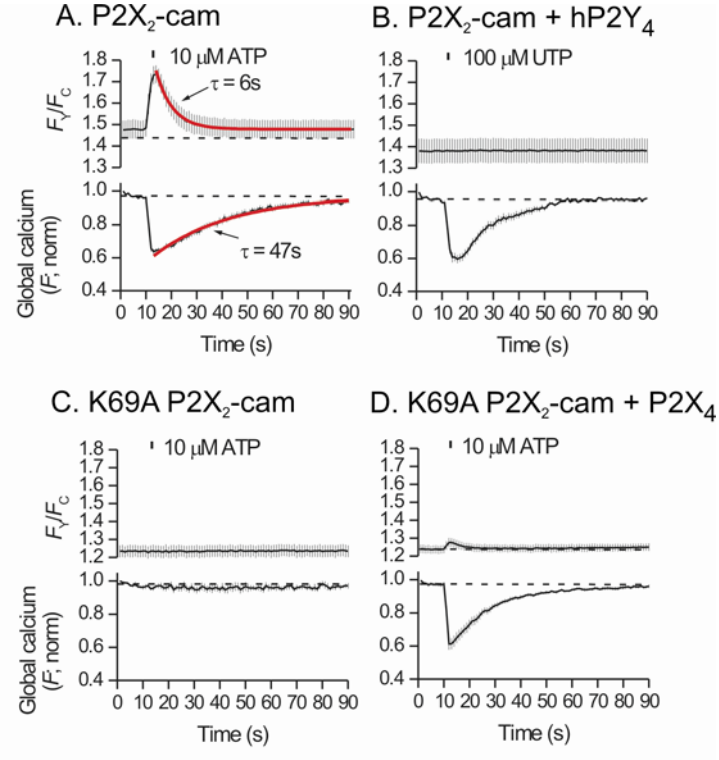

Supplementary note 1 Fig 1. Controls for ATP-evoked FRET changes for $P2X_2$-cam receptors.

A. Upper panel: FRET changes for $P2X_2$-cam receptors in response to a 1s application of 100 µM ATP. Lower panel: global changes in Ca^{2+} measured with Fura red. The red lines are single exponential fits to the decaying phases of the FRET and Fura red signals (see text for average data).

B-D. As in A, but for the indicated constructs.

References for Supplementary note 1:

1. Fisher, J. A., Girdler, G. & Khakh, B. S. Time resolved measurement of state specific P2X ion channel cytosolic gating motions. J Neurosci 24, 10475-10487 (2004).

2. Egan, T. M. & Khakh, B. S. Contribution of calcium ions to P2X channel responses. J Neurosci 24, 3413-20 (2004).
3. Torres, G., Egan, T. & Voigt, M. Hetero-oligomeric Assembly of P2X Receptor Subunits. Specificities exist with regard to possible partners. *J Biol Chem* 274, 6653-6659 (1999).
4. Miyawaki, A., Griesbeck, O., Heim, R. & Tsien, R. Y. Dynamic and quantitative Ca2+ measurements using improved cameleons. Proc Natl Acad Sci U S A 96, 2135-2140 (1999).
5. Khakh, B. S. & North, R. A. P2X receptors as cell surface ATP sensors in health and disease. Nature 442, 527-32 (2006).
6. Michalet, X. et al. The power and prospects of fluorescence microscopies and spectroscopies. Annual Review of Biophysics and Biomolecular Structure 32, 161-182 (2003).
7. Khakh, B. S., Fisher, J. A., Nashmi, R., Bowser, D. N. & Lester, H. A. An angstrom scale interaction between plasma membrane ATP-gated P2X2 and a4b2 nicotinic channels measured with FRET and TIRF microscopy. J Neurosci 20, 6911-20 (2005).
8. North, R. A. Molecular physiology of P2X receptors. Physiol Rev 82, 1013-1067 (2002).
9. Kucenas, S., Soto, F., Cox, J. A. & Voigt, M. M. Selective labeling of central and peripheral sensory neurons in the developing zebrafish using P2X(3) receptor subunit transgenes. Neuroscience 138, 641-52 (2006).
10. Koster, R. W. & S.E. Fraser. Tracing transgene expression in living zebrafish embryos. . Dev Biol. 233, 329-46 (2001).
11. Sagasti, A., Guido, M. R., Raible, D. W. & Schier, A. F. Repulsive interactions shape the morphologies and functional arrangement of zebrafish peripheral sensory arbors. Curr Biol 15, 804-14 (2005).
12. Khakh, B. S. et al. Activation-dependent changes in receptor distribution and dendritic morphology in hippocampal neurons expressing P2X2-green fluorescent protein receptors. Proc Natl Acad Sci U S A 98, 5288-5293 (2001).
13. Migita, K., Haines, W. R., Voigt, M. M. & Egan, T. M. Polar residues of the second transmembrane domain influence cation permeability of the ATP-gated $P2X_2$ receptor. J Biol Chem 276, 30934-41 (2001).
14. Hille, B. Ion channels of excitable membranes. Third edition. Sinauer Associates Inc. Sunderland Massachusetts, USA. (2001).
15. Lippincott-Schwartz, J., Snapp, E. & Kenworthy, A. Studying protein dynamics in living cells. Nat Rev Mol Cell Biol 2, 444-56 (2001).

Supplementary note 2. Estimating the distance between the pore and Ca^{2+} reporter.

The experiments in the main text are consistent with the view that Ca^{2+} entry through P2X channels evokes FRET changes for the attached YC3.1 reporters on the C tail tip. What is the distance between the inner aspect of the pore and the reporter? To date there is no crystal structure of a P2X channel[5], and no similar ion channels of known structure with an equivalent cytosolic domain, vitiating precise measures of distance. However, we made inroads and estimated the distance by exploiting FRET as a molecular calliper[6]. We thus engineered $P2X_2$ receptors to carry CFP on the N terminus and YFP on the C tail in place of YC3.1 (CFP-$P2X_2$-YFP constructs; see Fig 1 below). Because the $P2X_2$ pore is formed by TM1 and TM2[5] this places the short N terminus (with attached CFP) near the inner opening of the pore, and the YFP at the C tail tip (see cartoon in Fig 1 below). CFP-$P2X_2$-YFP constructs were functional, with ATP-evoked currents similar to *wt* $P2X_2$, although the EC_{50} was shifted slightly to the right by ~3-fold. Moreover, CFP-$P2X_2$-YFP underwent robust FRET with efficiency at ~23% (see Fig). The Forster equation[6] presents the relationship between FRET efficiency (*e*) and distance as,

$$e = R_O^6 / (R_O^6 + R^6),$$

where, R_O is the characteristic distance for CFP/YFP when efficiency is 50% (~5nm) and R is the measured distance between CFP/YFP. This equation has several important assumptions, notably the fluorophore mutual orientations, which have been discussed by us and others[6, 7], but nonetheless can be used to provide a measure of the proximity between CFP and YFP in CFP-$P2X_2$-YFP channels, at ~6nm. These data and analysis thus indicate that YC3.1 is within a nanodomain of the inner aspect of the pore of $P2X_2$ channels, and thus in an optimal position to sense Ca^{2+} ions as they flow when the pore opens.

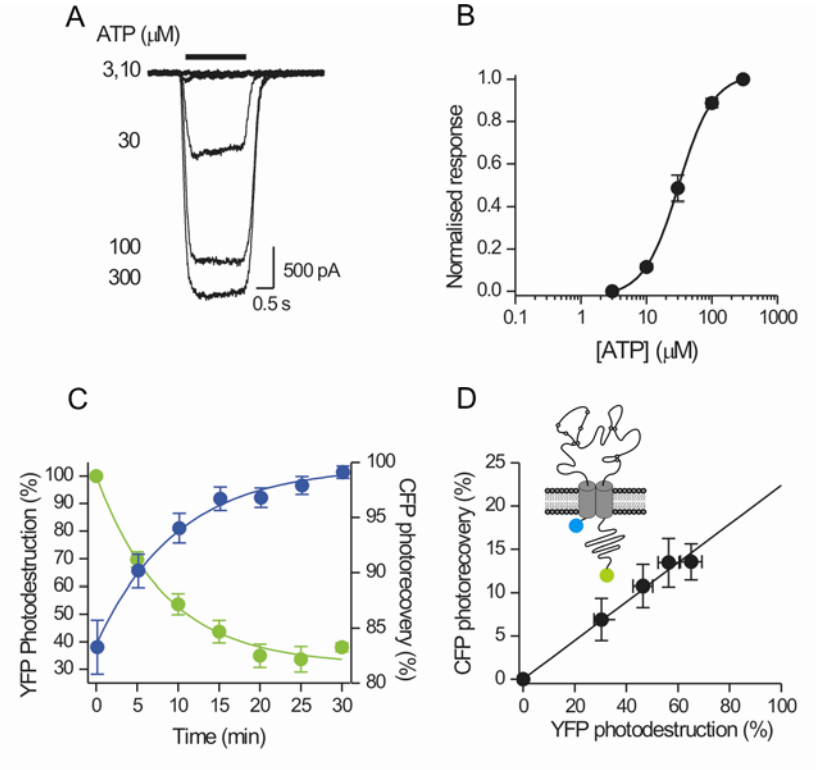

Supplementary note 2 Fig 1. Estimates of the distance between the pore and calcium sensor for P2X$_2$-cam receptors.
A. Representative traces for ATP-evoked currents from HEK cells expressing CFP-P2X$_2$-YFP receptors. **B.** Concentration-response curves for CFP-P2X$_2$-YFP receptors expressed in HEK cells. **C.** Photodestruction (green) of YFP and photorecovery (blue) of CFP during 525nm illumination of HEK cells expressing CFP-P2X$_2$-YFP receptors; note the similar time courses. **D.** Cartoon shows the location of CFP and YFP in CFP-P2X$_2$-YFP receptors, and the graph shows the determination of FRET efficiency for this construct at ~23%.

References for Supplementary note 2:

1. Khakh, B. S. & North, R. A. P2X receptors as cell surface ATP sensors in health and disease. Nature 442, 527-32 (2006).
2. Michalet, X. et al. The power and prospects of fluorescence microscopies and spectroscopies. Annual Review of Biophysics and Biomolecular Structure 32, 161-182 (2003).
3. Khakh, B. S., Fisher, J. A., Nashmi, R., Bowser, D. N. & Lester, H. A. An angstrom scale interaction between plasma membrane ATP-gated P2X2 and a4b2 nicotinic channels measured with FRET and TIRF microscopy. J Neurosci 20, 6911-20 (2005).

Supplementary methods

Molecular biology. YC3.1 (kind gift from Roger Y. Tsien) was amplified by PCR with flanking 5' *Xho1* and 3' *Xba1* sites. The PCR product was subcloned into $P2X_2$-YFP that we have previously reported[1], by excising the YFP with *Xho1*/*Xba1*. The resulting plasmid ($P2X_2$-cam) was verified by sequencing. $P2X_1$-cam, $P2X_3$-cam, $P2X_4$-cam, $P2X_5$-cam, $P2X_6$-cam and $P2X_7$-cam were made using the same strategy using the cognate YFP tagged receptors that were available in the lab as a result of previous published[1] and unpublished work. The K69A mutation was made using the Quickchange Site Directed mutagenesis kit (Stratagene), and verified by sequencing.

HEK 293 cell culture. HEK 293 cells (obtained from ATCC) were maintained in 75 cm^2 cell culture flasks in DMEM/F12 media with Glutamax (Invitrogen) supplemented with 10% fetal bovine serum and penicillin/streptomycin. Cells were grown in a humidified atmosphere of 95% air / 5% CO_2, at 37 ºC in a cell culture incubator. The cells were split 1 in 10 when confluence reached 60-90%, which was generally every 3 to 4 days. Cells were prepared for transfection by plating onto 6-well plates at the time of splitting, 3-4 days before transfection. They were transfected at 60-90% confluence. For transient expression in HEK-293 we used 0.5-1 μg plasmid cDNA and the Effectene transfection reagent (Qiagen) for each well of a 6 well plate. The manufacturer's instructions were followed, with 4 μl of enhancer and 10 μl of Effectene used for each transfection. The transfection efficiency was 40-60%. For some experiments appropriately transfected HEK cells were loaded for one hour with 5μM Fura-red AM with 0.05% pluronic acid (Molecular Probes) in the dark, washed in HEK cell buffer and left in the dark for a further one hour before experimentation on the epifluorescence rig.

Western blotting. Total proteins from HEK cell lysates were used for Western blotting**.** For each construct, HEK cells were transfected with ~0.5 μg of cDNA in 35 mm dishes, and 24 hours later the

cells were suspended in cell lysis buffer containing 20 mM HEPES pH 7.4, 100 mM NaCl, 1 mM DTT, 1% triton X-100 and a protease inhibitor cocktail. Cells were triturated with a 26 g needle and incubated in the lysis buffer for 30 min at 4ºC. This mixture was then centrifuged at 13000 rpm for 30 min at 4ºC, and soluble proteins in the supernatant were transferred into a clean tube. Equal amounts of proteins (~20 μg) were loaded on 10% NuPAGE novex Bis-tris gels (Invitrogen), using Invitrogen NuPAGE LDS sample preparation buffer supplemented with 0.5% β-mercaptoethanol. Gels were run in NuPAGE MES running buffer (Invitrogen) at 130 V for 2 h. Protein transfer was achieved using NuPAGE transfer buffer (Invitrogen), for 1 h at 30 V, on Hybond ECL nitrocellulose membrane (Amersham Biosciences). After transfer, nitrocellulose membranes were blocked PBS containing 0.05% Tween and 5% milk for 2 hrs, and incubated overnight with rabbit anti-GFP antibody (1/2000 dilution; Molecular Probes) or with mouse anti-FLAG M2 antibody (1/1000 dilution; Sigma). After washing 3 times for 10 minutes each in PBS/Tween the membranes were incubated with anti-rabbit or ant-mouse HRP secondary antibodies (Zymed, 1/5000 dilution), in PBS containing 0.5% BSA, for 1 hr at room temperature. Membranes were washed 3 times for 10 mins each in PBS/Tween, and the protein bands imaged using ECL reagent (GE Healthcare).

Patch-clamp electrophysiology. HEK 293 cells were used for recordings 24–48 h post transfection as described by us [1]. The cells were gently mechanically dispersed and plated onto glass coverslips 2-12 hrs before use[1]. The extracellular recording solution comprised (mM) NaCl 147, KCl 2, $MgCl_2$ 1, $CaCl_2$ 1, HEPES 10 and glucose 10 (pH 7.4), and the pipette solution (mM) KCl (or CsCl, or NaCl) 154, EGTA 11 and HEPES 10. In some cases the EGTA concentration was reduced to 0.1mM. Whole-cell voltage clamp recordings were made with 3-5 MΩ borosilicate glass electrodes (WPI), using an Axopatch 200B or 700A amplifier controlled by a computer running pCLAMP 8.1 software via a Digidata 1322A

interface (Axon Instruments). Data were filtered at 2-5 kHz and digitized at >5 kHz. The chamber housing the glass coverslip was perfused with extracellular buffer at a rate of 2–3 ml/min.

TIRF-FRET microscopy. Briefly[1], we used an Olympus IX71 microscope equipped with an Andor IXON DV887DCS EMCCD camera. The control of excitation and image acquisition was achieved using TILLVision software. The beams of 454/488/515 nm Argon (100 mW) and 442 nm solid state (45 mW) lasers were combined and controlled with a TILL Polyline laser combiner, TIRF dual port condenser and acoustoptical tuneable filter and controller (AOTF; all from TILL Photonics) and fed into a Kineflex broad band fiber for entry into the TIRF condenser. We used an Olympus 60X 1.45 NA lens to achieve TIRF. For FRET we used the 442 nm laser line, and a beam splitter inserted in the emission path of the microscope.

Fluorescence recovery after photobleaching (FRAP) microscopy. FRAP was carried out using an Olympus BX61WI and FV300 Fluoview confocal laser scanning microscope. Bleaching was achieved with 100% laser power for ~1s, followed by examination of recovery every 0.3s with the laser power at 0.1% of maximum. For these experiments we used the 488 nm laser line of a Argon laser and a 40X objective lens with a NA of 0.8 (Olympus).

Hippocampal neuron cultures. Hippocampal neurons were prepared as described by us[7]. We used young animals because they do not express endogenous P2X receptors at this stage of development[8], thus allowing precise interpretations to be made for the experiments where we transfected recombinant receptors. Briefly, typically five rat pups at E19 or P1 were used for hippocampal cultures. The mother was euthanized following institutional procedures, and the embryos removed to ice cold dissection medium comprising Earles Buffered Salt Solution (EBSS; with no Ca^{2+} or Mg^{2+} and no phenol red; Invitrogen), HEPES (10 mM, pH 7.4; Sigma) and penicillin/streptomycin (1/100 dilution; Invitrogen).

Hippocampi were dissected in Petri dishes filled with ice-cold medium. The dissected hippocampi (in medium, on ice) were cut in half and then transferred to a 15 ml tube with 10 U/ml papain PAP2 powder (Worthington PAPAIN-022; Lakewood NJ), and incubated for 15 min at 37°C. Once the pieces of tissue had settled, digestion solution was removed and 10 ml of cold culture medium was added. This step was repeated and then the pieces were triturated 5/6 times in a 2 ml volume of ice cold culture medium, with paired flame-polished pipettes of progressively smaller bores. A hemacytometer was used to quantify yield (typically 2.5 million neurons per ml) and ~200,000 neurons were used for plating onto each coverslip. The coverslips were previously coated with poly-D-lysine (50 μg/ml; Sigma) and then overnight with 150 μl of 20 μg/ml laminin (Sigma) in sterile dissection medium. Three hours after plating the cells were fed with 2 ml of pre-warmed culture medium, and fed again one day after plating by substituting 1 ml of fresh pre-warmed medium for 1 ml of existing medium. The culture medium comprised, MEM with no phenol red (Invitrogen), glucose (20 mM), penicillin/streptomycin (Invitrogen), Na pyruvate (2 mM; Sigma), HEPES (25 mM; Sigma), N2 supplement (1 in 100 dilution; Invitrogen) and heat-inactivated horse serum (10%; Invitrogen). Three to four days after plating the media was replaced with Neurobasal. The neurons were used for experiments within 14 days. The Neurobasal media comprised, neurobasal 500 ml, 10 ml B27 Supplement, 5ml Pen/Strep and 1.25 ml L-glutamine (all from Gibco).

Neuron transfection. We used an optimized protocol that gives healthy neurons with transfection rates suitable for electrophysiology and imaging (~50 transfected neurons per cover slip). We transfected the neurons at 7-10 DIV. The neurons were in Neurobasal medium at this point,and were fed every Tuesday and Friday. The transfection was done on the day of feeding. On this day half the media was removed (1ml from each well of a 6-well plate housing 3 coverslips) and the neurons fed with fresh Neurobasal (1 ml), that had been pre equilibrated in the cell culture incubator (37°C; 5% CO_2) for at least 2 hr. The

removed media was supplemented with an equal volume of new media and stored in a vented flask in the cell culture incubator (this is the 'the fed and conditioned media'). We used lipofectamine2000 (L2K) from Invitrogen for the transfection. For 1 well of 6 well plate housing three 13 mm coverslips, we added 6μl of DNA (at ~300ng/μl) to 100 μl of MEM. In a separate tube we added 4 μl of L2K with 100 μl of MEM (kept for 5 min at room temp). Then we added the 100 μl of the L2K/MEM mix to the DNA/MEM mix, flicked the tube and incubate at RT for 20 min. This was added dropwise to the neurons after which the plates given a gentle swirl and returned to the incubator. After 6-8 hrs all the medium was removed from each well and replaced with 2 ml of the "fed and conditioned medium" from earlier. The important parameters were good quality DNA (~300 ng/ul) and cells being changed into Neurobasal medium in the first week after plating. We imaged the cells between ~3 days post-transfection.

Molecular biology and imaging of zebrafish. To clone a putative promoter for the $P2X_{3A}$ gene, we PCR amplified a 1665 bp fragment from *Fugu rubripes* genomic DNA immediately upstream of the $P2X_{3A}$ translation start site (primers: GGAGGTGTTCCCAACTGGTC and GCACCAGAGAGCCAATATCTTG). *Fugu* was chosen because of its more compact genome and close evolutionary relationship to zebrafish. In control experiments, this fragment drove GFP expression almost exclusively in trigeminal and RB sensory neurons, a finding consistent with other work on the $P2X_3$ promoter[9]. The putative $P2X_3$ promoter was subcloned upstream of a Gal4-VP16 fusion protein (fr$P2X_{3A}$-Gal4VP16). The $P2X_2$-cam reporter and the control K69A $P2X_2$-cam were each subcloned into separate vectors downstream of the Gal4 Upstream Activating Sequence (UAS). Approximately 15 pg of the f$P2X_{3A}$-Gal4VP16 driver construct along with 15 pg of either the UAS-$P2X_2$-cam or the UAS-K69A $P2X_2$-cam reporter constructs were microinjected into wild-type zebrafish embryos before the 4-cell stage. The GAL4VP16/UAS system provided amplification that enhanced expression of the reporters[10, 11]. To visualize Rohon-Beard axons expressing the reporter, embryos were mounted in 1% agarose at

approximately 54 hours-post-fertilization (hpf) and imaged on a Zeiss LSM 510 confocal microscope using a 20x water immersion objective. Approximately 10 to 20 confocal sections (~5 μm each) were compiled into a 3-D projection using Zeiss software. FRET experiments were performed on the epifluorescence FRET rig that is described in detail in preceding sections. For these experiments the fish were mounted in agarose blocks and bathed in local anesthetic (tricaine 0.02%).

Agonist applications. Drugs were applied to single cells using fast applications or in the bathing medium (at 2-3 ml/min). We have described the rapid agonist application devices that we used[1]. Briefly, receptor activation on the neurites[12] and zebrafish sensory neurons was achieved with local puffs[12] with a Picospritzer III (General Valve Company; Fairfield NJ USA), whereas a local fast perfusion device (SF-77B Perfusion Fast Step; Warner Instruments) was used for activating all the receptors on HEK cells[2]. In both cases solution change occurred in ~6-10ms, and the puffing pipettes were positioned with a micromanipulator.

Electrical field stimulation. We used a microscope stage mounted glass bottom chamber with built in platinum electrodes (Warner Instruments) connected to a Grass S88 stimulator for field stimulation. We used a pulse width of ~1ms, and stimulation frequency of 30 Hz, and varied the duration of the stimulus train to trigger between 1-90 action potentials. The stimulus strength was chosen arbitrarily to be the smallest that would trigger a F_Y/F_C response.

Data analysis. Ca^{2+} permeability was determined using previously described methods[13]. First, we determined the ATP-evoked current reversal potential using equal concentrations of Cs^+ in the intra- and extracellular solutions (154 mM). Then we changed the extracellular solution to contain 112 mM Ca^{2+}, and determine the reversal potential of the ATP-evoked current again (using 1 mM ATP). We calculated the relative permeability of Ca^{2+} to Cs^+ (pCa^{2+}/pCs^+) as

$$pCa^{2+}/pCs^{+}=(a_{Cs}[Cs^{+}]_i.\exp(\Delta E_{rev}F/RT)(1+\exp(\Delta E_{rev}F/RT))4a_{Ca}[Ca^{2+}]_o,$$

where ΔE_{rev} is the change in reversal potential on switching from Cs^{+} to Ca^{2+}, aCs is the activity coefficient of Cs^{+} (0.75), aCa is the activity coefficient of Ca^{2+} (0.25), F is Faradays constant, R universal gas constant and T absolute temperature[14]. For donor de-quenching experiments the FRET efficiency (*e*) was calculated as

$$e = (1 - [I_{C-before} / I_{C-after}]) \times 100,$$

where $I_{C\text{-}before}$ is the donor fluorescence intensity before photo destruction and $I_{C\text{-}after}$ is the intensity after photo destruction. The photo destruction of the YFP proceeds with a rate equivalent to the de-quenching of the donor, and plotting the photo recovery versus photo destruction yields a linear plot. We used such linear plots and extrapolated to 100% acceptor photodestruction to calculate the maximum donor de-quenching for epifluorescence microscopy: *e* is given by the Y-axis intercept. F_Y/F_C traces and movies were made using the Cairn Optosplit Applet in Image J. Concentration response curves were fit to the Hill equation in Origin 7.5, and charge transfer was measured by integration of the current traces in Clampfit 10.1 or Origin. Single exponential fits (Origin 7.5) were used to measure the FRAP time constant (τ), and the apparent diffusion coefficient was estimated[15] using the function

$$D = 0.224 \times r^2 / t_d,$$

where *r* is the radius of the area that was bleached and t_d is the time taken for FRAP to recover to half its final value ($ln2.\tau$). The average distance (*d*) traveled in one dimension in time (*t*) was estimated as

$$d = \sqrt{2Dt}$$

Software and statistical analysis. Electrophysiological analysis was performed with Clampfit 10.1 (Molecular Devices Axon Instruments) or Origin 6.1 or 7.5 (OriginLab Corp) and all statistical tests were run in GraphPad Instat 3.0 (GraphPad Software). Image analysis was performed with ImageJ (NIH). Data are as mean ± S.E.M. from at least 6 experiments.

References for Supplementary Methods:

1. Fisher, J. A., Girdler, G. & Khakh, B. S. Time resolved measurement of state specific P2X ion channel cytosolic gating motions. J Neurosci 24, 10475-10487 (2004).
2. Khakh, B. S., Fisher, J. A., Nashmi, R., Bowser, D. N. & Lester, H. A. An angstrom scale interaction between plasma membrane ATP-gated P2X2 and a4b2 nicotinic channels measured with FRET and TIRF microscopy. J Neurosci 20, 6911-20 (2005).
3. North, R. A. Molecular physiology of P2X receptors. Physiol Rev 82, 1013-1067 (2002).
4. Kucenas, S., Soto, F., Cox, J. A. & Voigt, M. M. Selective labeling of central and peripheral sensory neurons in the developing zebrafish using P2X(3) receptor subunit transgenes. Neuroscience 138, 641-52 (2006).
5. Koster, R. W. & S.E. Fraser. Tracing transgene expression in living zebrafish embryos. . Dev Biol. 233, 329-46 (2001).
6. Sagasti, A., Guido, M. R., Raible, D. W. & Schier, A. F. Repulsive interactions shape the morphologies and functional arrangement of zebrafish peripheral sensory arbors. Curr Biol 15, 804-14 (2005).
7. Khakh, B. S. et al. Activation-dependent changes in receptor distribution and dendritic morphology in hippocampal neurons expressing P2X2-green fluorescent protein receptors. Proc Natl Acad Sci U S A 98, 5288-5293 (2001).
8. Egan, T. M. & Khakh, B. S. Contribution of calcium ions to P2X channel responses. J Neurosci 24, 3413-20 (2004).
9. Migita, K., Haines, W. R., Voigt, M. M. & Egan, T. M. Polar residues of the second transmembrane domain influence cation permeability of the ATP-gated $P2X_2$ receptor. J Biol Chem 276, 30934-41 (2001).
10. Hille, B. Ion channels of excitable membranes. Third edition. Sinauer Associates Inc. Sunderland Massachusetts, USA. (2001).
11. Lippincott-Schwartz, J., Snapp, E. & Kenworthy, A. Studying protein dynamics in living cells. Nat Rev Mol Cell Biol 2, 444-56 (2001).